Hindawi
Journal of Advanced Transportation
Volume 2020, Article ID 8898923, 16 pages
https://doi.org/10.1155/2020/8898923

Research Article

Estimation of Disease Transmission in Multimodal Transportation Networks

Yu Zheng

School of Economic and Management, Tongji University, Shanghai 200092, China

Correspondence should be addressed to Yu Zheng; 1710270@tongji.edu.cn

Received 27 March 2020; Revised 21 May 2020; Accepted 16 June 2020; Published 1 August 2020

Academic Editor: Weiwei Qi

Mathematical models are important methods in estimating epidemiological patterns of diseases and predicting the consequences of the spread of diseases. Investigation of risk factors of transportation modes and control of transportation exposures will help prevent disease transmission in the transportation system and protect people's health. In this paper, a multimodal traffic distribution model is established to estimate the spreading of virus. The analysis is based on the empirical evidence learned from the real transportation network which connects Wuhan with other cities. We consider five mainstream travel modes, namely, auto mode, high-speed railway mode, common railway mode, coach mode, and flight mode. Logit model of economics is used to predict the distribution of trips and the corresponding diseases. The effectiveness of the model is verified with big data of the distribution of COVID-19 virus. We also conduct model-based tests to analyze the role of lockdown on different travel modes. Furthermore, sensitivity analysis is implemented, the results of which assist in policy-making for containing infection transmission through traffic.

1. Introduction

Despite tremendous efforts to reduce and control infectious diseases, infections continue to be a global threat to worldwide public health. Understanding the virus propagation is quite essential for the implementation of antivirus methods. While research studies about the antivirus policy have been extensively investigated, the viewpoint from the perspective of the propagation along transportation modals is relatively ignored. Consideration of risk factors of transportation modes and control of transportation exposures will help prevent disease transmission in the transportation system and protect people's health. When an infectious disease case occurs at a location, investigators need to understand the mechanisms of disease propagation in the transportation network.

On December 31, 2019, the outbreak of novel coronavirus was first reported in China. The global outbreak of COVID-19 was mainly caused by transmission through different transportation modes. To prevent the spreading of virus, all the transportation system from Wuhan to the outside was closed in the morning of January 23, 2020. On January 30, 2020, the WHO (World Health Organization) declared a global emergency. On March 11, WHO declared the COVID-19 outbreak to be a global pandemic. For weeks after the first reports of a mysterious new virus of COVID-19, millions of people poured out of the central Chinese city, cramming onto buses, trains, and planes as the first wave of China's great Lunar New Year migration broke across the nation, and some of them are virus carriers. The travel patterns broadly track with the early spread of the virus. The majority of confirmed cases and deaths have occurred in China, within Hubei province, followed by high numbers of cases in central China, with pockets of infections in Chongqing, Shanghai, and Beijing as well. The initial spread of travelers to provinces in central China is with large pools of migrant workers. There might be a "high correlation" between the early spread of coronavirus cases and the distribution of travel destinations. The atmosphere in the transportation vessels is closed, and it is easy for the virus to spread. And the transmission speed is different in different traffic modals, due to the different air fluency in the traffic vessels.

Mathematical models have become important tools in epidemiology in understanding epidemiological patterns of diseases and predicting the consequences of the introduction of public health interventions to control the spread of diseases. There are two lines of studies in epidemics spreading. The first line is the spreading model of differential equation, and the second line is the complex network theory. In the literature, there are three spreading models widely used in modeling virus transmission, namely, SIR model, SIS model, and SI model (acronyms such as M, S, E, I, and R are often used for the epidemiological classes. The class M represents individuals with passive immunity. The class S represents susceptible individuals who can become infected. The class E represents the exposed individuals in the latent period, who are infected but not yet infectious. The class I represents the individuals of infective, who are infectious in the sense that they are capable of transmitting the infection. The class R represents recovered individuals with permanent infection-acquired immunity. The choice of which epidemiological class to include in a model depends on the characteristics of the particular disease being modeled and the purpose of the model) [1–4]. To solve the models, three kinds of algorithms have been developed based on percolation theory [5, 6], mean field theory [7, 8], and Markov chain theory [9, 10].

Researchers also developed models to investigate the propagation of different types of viruses including some nonbiological viruses, such as the computer virus, the flash disk virus, the Bluetooth phone virus, and the email virus. Otero-Muras et al. presented a systematic approach to the biochemical network dynamic analysis and control based on both thermodynamic and control theoretic tools [11]. Based on biological control strategy in pest management, Pang and Chen constructed a pest-epidemic model with impulsive control, i.e., periodically spraying microbial pesticide and releasing infected pests at different fixed moments [12]. Jin and Wang developed a new dynamic propagation model of FD-SEIR, namely, flash disk virus susceptible-exposed-infectious-recovered, which is embodied by introducing the FD state and new propagation rate [13]. Huang et al. developed an epidemic model of Bluetooth phone virus [14]. Li et al. formulated a novel deterministic SEIS model for the transmission of email viruses in growing communication networks [15]. Jackson and Chen-Charpentier presented two plant virus propagation models, one with no delays and the other with two delays [16]. Jia and Lv established a stochastic rumor propagation model. Sufficient conditions for extinction and persistence in the mean of the rumor have been examined [17]. Zhang et al. established a spreading model based on contact strength and SI model, and a weighted network with community structure based on a network model proposed by Barrat et al. [18].

In the following, a multimodal traffic distribution model is established to estimate the spreading of virus. The analysis is based on the empirical evidence learned from the real transportation network which connects Wuhan with other cities. Five travel modes are considered, namely, auto mode, high-speed railway mode, common railway mode, coach mode, and flight mode. Logit model of economics is used to predict the distribution of trips and the corresponding diseases. The effectiveness of the model is verified with big data of the distribution of COVID-19 virus. The main contributions of the paper are in four aspects. First, we propose a multimodal traffic distribution model using data of the real transportation system. Second, we study the relation between the state of disease transmission and the traffic flows distribution based on the numerical results of the proposed model and the big data of the distribution of COVID-19 virus. Third, we use the model to predict the role of lockdown on different transport means and analyze its impact on the disease transmission. Fourth, we present a sensitivity analysis for the proposed model and derive various transportation improvement policies to control large-scale transportation exposure.

The remainder of this paper is organized as follows. Section 2 establishes a multimodal traffic distribution model to estimate the spreading of virus. The proposed model is validated in Section 3, using a real traffic distribution from Wuhan to other regions in China during the outbreak of COVID-19. Conclusions are made in Section 4.

2. Multimodal User Equilibrium Model

2.1. Multimode Travel Cost Functions. The multimode travel cost functions are based on the empirical evidence learned from the real transportation network connecting Wuhan to other cities. We consider five mainstream travel modes, namely, auto mode, high-speed railway mode, common railway mode, coach mode, and flight mode (Tables 1 and 2). Let c_m^d represent the travel cost in the travel mode m ($m \in M, M = \{$auto, high–speed railway, common railway, coach, flight$\}$) to a destination region indexed by a region name d ($d \in D$, $D = \{$Xiaogan, Huanggang, Jingzhou, Xianning, E'zhou, Xiangyang, Huangshi, Jingmen, Suizhou, Xiantao, Yichang, Tianmen, Shiyan, Enshi, Qianjiang, Henan, Hunan, Anhui, Jiangxi, Guangdong, Jiangsu, Chongqing, Sichuan, Shandong, Zhejiang, Hebei, Fujian, Beijing, Guangxi, Shanxi, Shanghai, Shanxi, Guizhou, Yunnan, Hainan, Gansu, Liaoning, Heilongjiang, Xinjiang, Inner Mongolia, Jilin, Tianjin, Ningxia, Qinghai, Tibet, Hong Kong, Macao, Taiwan$\}$). The set of destination regions D includes 15 cities within the province of Hubei and 33 province-level regions in China. We further define the set of 15 cities within the province of Hubei as D_{in} ($D_{\text{in}} = \{$Xiaogan, Huanggang, Jingzhou, Xianning, E'zhou, Xiangyang, Huangshi, Jingmen, Suizhou, Xiantao, Yichang, Tianmen, Shiyan, Enshi, Qianjiang$\}$) and the set of other 33 province-level regions as D_{out} ($D_{\text{out}} = \{$Henan, Hunan, Anhui, Jiangxi, Guangdong, Jiangsu, Chongqing, Sichuan, Shandong, Zhejiang, Hebei, Fujian, Beijing, Guangxi, Shanxi, Shanghai, Shanxi, Guizhou, Yunnan, Hainan, Gansu, Liaoning, Heilongjiang, Xinjiang, Inner Mongolia, Jilin, Tianjin, Ningxia, Qinghai, Tibet, Hong Kong, Macao, Taiwan$\}$), and $D = D_{\text{in}} \cup D_{\text{out}}$.

The function of travel cost for each mode from Wuhan to a destination region indexed by d is described as follows:

Table 1: Automobile transportation parameters.

City	Province	Time	Distance	Toll	Gas fee
Xiaogan	Hubei	90	76.5	30	43
Huanggang	Hubei	77	75.3	30	42
Jingzhou	Hubei	180	220	90	123
Xianning	Hubei	90	92.6	30	52
E'zhou	Hubei	90	75	20	42
Xiangyang	Hubei	227	313	150	175
Huangshi	Hubei	100	100	40	56
Jingmen	Hubei	180	240	110	134
Suizhou	Hubei	120	170	80	95
Xiantao	Hubei	110	102	40	57
Yichang	Hubei	240	322	140	180
Tianmen	Hubei	120	142	50	80
Enshi	Hubei	420	519	250	291
Shiyan	Hubei	300	443	210	248
Qianjiang	Hubei	131	155	70	87
Shijiazhuang	Hebei	660	898	440	503
Taiyuan	Shanxi	720	944	450	529
Shenyang	Liaoning	1320	1812	890	1015
Changchun	Jilin	1560	2088	1030	1169
Harbin	Heilongjiang	1440	2354	1160	1318
Nanjing	Jiangsu	408	550	260	308
Hangzhou	Zhejiang	660	827	350	463
Hefei	Anhui	300	388	180	217
Fuzhou	Fujian	672	919	450	515
Nanchang	Jiangxi	330	355	170	199
Ji'nan	Shandong	600	864	420	484
Zhengzhou	Henan	360	514	250	288
Changsha	Hunan	289	345	150	193
Guangzhou	Guangdong	672	955	480	535
Haikou	Hainan	1152	1566	750	877
Chengdu	Sichuan	840	1130	550	633
Guiyang	Guizhou	720	1011	510	566
Kunming	Yunnan	1170	1558	760	872
Xi'an	Shanxi	510	740	360	414
Lanzhou	Gansu	930	1360	670	762
Xi'ning	Qinghai	1188	1594	790	893
Taibei	Taiwan	—	—	—	5600
Beijing	—	780	1174	580	657
Tianjin	—	720	1144	560	641
Shanghai	—	606	825	390	462
Chongqing	—	690	897	440	502
Hohhot	Inner Mongolia	960	1380	650	773
Nanning	Guangxi	810	1209	590	677
Lhasa	Tibet	3060	3482	1110	1950
Yinchuan	Ningxia	966	1448	710	811
Urumqi	Xinjiang	2160	3267	1600	1830
Hong Kong	—	840	1107	510	620
Macao	—	960	1210	600	678

Note that, in this part, the unit of measurement is kilometers for the distance, minutes for the time, and CNY for all kinds of tolls and fees.

(1) Auto mode:

$$c_{\text{auto}}^{d} = \left(\frac{vot_{\text{auto}} T_{\text{auto}}^{d} + \varepsilon_{\text{auto}} l_{d} + P_{\text{highway}}^{d}}{n} \right), \quad \forall d \in D, \quad \text{(1a)}$$

where $\varepsilon_{\text{auto}}$ represents the cost of gasoline consumed per kilometer and T_{auto}^{d} denotes the auto travel time. The cost function c_{auto}^{d} consists of three terms. The first one stands for the monetary cost of travel time captured by the product of the value of in-vehicle travel time vot_{auto} and the travel time T_{auto}^{d}; the second one is the cost of gasoline consumed by this trip; the third one is the highway tolls charged along the highway captured by the product of the highway toll charged per kilometer and the total highway length. The average vehicle occupancy n is the average number of occupants in a vehicle. We set the n-piece of auto utility function taking account of the actual traffic situation. The Transport Bureau of

Table 2: Transportation parameters of high-speed railway, common railway, coach, and flight.

City	Province	High-speed railway		Common railway		Coach		Flight	
		Time	Ticket fee	Time	Ticket fee	Time	Ticket fee	Time	Ticket fee
Xiaogan	Hubei	30	58	60	14.5	60	32	—	—
Huanggang	Hubei	90	22	37	20	—	—	—	—
Jingzhou	Hubei	90	76	89	32.5	300	60	—	—
Xianning	Hubei	24	40	60	12.5	60	28	—	—
E'zhou	Hubei	24	20	80	12.5	60	28	—	—
Xiangyang	Hubei	90	130	190	50.5	240	88	—	—
Huangshi	Hubei	37	30	100	16.5	120	42	—	—
Jingmen	Hubei	—	—	190	40.5	180	101	—	—
Suizhou	Hubei	55	70	128	26.5	180	66	—	—
Xiantao	Hubei	60	50	—	—	90	35	—	—
Yichang	Hubei	150	121	310	53.5	270	105	—	—
Tianmen	Hubei	60	45	90	19.5	180	55	—	—
Enshi	Hubei	270	187	420	78	480	130	—	—
Shiyan	Hubei	144	217	330	72	390	135	—	—
Qianjiang	Hubei	90	65	—	—	150	57	—	—
Shijiazhuang	Hebei	240	415	540	124	—	—	450	1450
Taiyuan	Shanxi	390	486	1332	173.5	750	320	105	727
Shenyang	Liaoning	660	800	1320	217	1440	480	180	1820
Changchun	Jilin	680	904	1527	243	—	—	180	1800
Harbin	Heilongjiang	753	1012	1396	268.5	—	—	180	1800
Nanjing	Jiangsu	180	200	—	—	480	200	—	—
Hangzhou	Zhejiang	300	300	720	120	700	285	80	830
Hefei	Anhui	120	134	—	—	360	150	—	—
Fuzhou	Fujian	371	267	720	120	700	280	90	870
Nanchang	Jiangxi	150	120	344	53.5	390	120	—	—
Ji'nan	Shandong	360	525	720	130	780	280	95	1000
Zhengzhou	Henan	140	244	300	75	480	140	—	—
Changsha	Hunan	92	165	240	53.5	300	120	—	—
Guangzhou	Guangdong	260	464	750	138.5	960	340	110	1800
Haikou	Hainan	—	—	1440	250	1290	430	150	1700
Chengdu	Sichuan	560	375	990	185	960	330	120	1350
Guiyang	Guizhou	300	481	930	163.5	960	320	115	1000
Kunming	Yunnan	420	665	1373	217	1500	480	135	1660
Xi'an	Shanxi	270	455	900	135.5	560	240	85	1200
Lanzhou	Gansu	400	654	1200	190	1200	430	135	1330
Xi'ning	Qinghai	—	—	—	—	—	—	130	1300
Taibei	Taiwan	—	—	—	—	—	—	155	1400
Beijing	—	270	520	720	152.5	900	320	120	2200
Tianjin	—	300	525	840	156.5	960	300	115	1150
Shanghai	—	300	336	900	140	720	250	95	1880
Chongqing	—	390	279	540	140	780	280	95	1650
Hohhot	Inner Mongolia	—	—	1828	229	—	—	130	1050
Nanning	Guangxi	450	478	840	170	1050	320	120	1180
Lhasa	Tibet	—	—	—	—	—	—	230	1070
Yinchuan	Ningxia	—	—	1560	198	—	—	135	1300
Urumqi	Xinjiang	—	—	2310	345	—	—	260	2000
Hong Kong	—	280	679	—	—	—	—	130	1574
Macao	—	—	—	—	—	—	—	100	1380

Note that, in this part, the unit of measurement is kilometers for the distance, minutes for the time, and CNY for all kinds of tolls and fees.

Wuhan announced that the average vehicle occupancy of a privately owned automobile in Wuhan is 1.8 persons/vehicle. Besides, it was reported by the Spring Festival Transport Office of the province of Hubei that advantages such as the trip cost shared by several relatives and friends, larger space for luggage, and no need to transfer are attracting more and more individuals traveling back home by a private car during the Spring Festival travel season. It is therefore reasonable to assume that the number of occupants in a vehicle within the Spring Festival travel season should be no less than the average vehicle occupancy, i.e., 1.8 persons/vehicle. Taking account of this, the value of n is set as 2.

(2) High-speed railway mode:

$$c^d_{\text{high-speed rail}} = vot_{\text{high-speed rail}} T^d_{\text{high-speed rail}} + \tau^d_{\text{high-speed rail}}, \quad \forall d \in D, \tag{1b}$$

where $T^d_{\text{high-speed rail}}$ is the high-speed railway travel time and vot_{rail} is the value of time spent in the high-speed railway. The travel cost $c^d_{\text{high-speed rail}}$ consists of 2 terms: the first term is the cost of the travel time and the second term represents the high-speed railway ticket price.

(3) Common railway mode:

$$c^d_{\text{rail}} = vot_{\text{rail}} T^d_{\text{rail}} + \tau^d_{\text{rail}}, \quad \forall d \in D, \tag{1c}$$

where T^d_{rail} is the common railway travel time and vot_{rail} is the value of time spent in the common railway. The travel cost c^d_{rail} consists of 2 terms: the first term is the cost of the travel time and the second term represents the common railway ticket price.

(4) Coach mode:

$$c^d_{\text{coach}} = vot_{\text{coach}} T^d_{\text{coach}} + \tau^d_{\text{coach}}, \quad \forall d \in D, \tag{1d}$$

where T^d_{coach} is the coach travel time and vot_{coach} is the value of time spent in a coach. The travel cost c^d_{coach} consists of 2 terms: the first term is the cost of the travel time and the second term represents the coach ticket price.

(5) Flight mode:

$$c^d_{\text{flight}} = vot_{\text{flight}} T^d_{\text{flight}} + \tau^d_{\text{flight}}, \quad \forall d \in D, \tag{1e}$$

where T^d_{flight} is the travel time by taking a plane and vot_{bus} is the value of time spent in a flight. The travel cost c^d_{flight} consists of 2 terms: the first term is the cost of the travel time and the second term is the flight ticket price.

2.2. Multimodal User Equilibrium Model. To cater for the consideration of both mode choice and destination choice, we propose a multimodal network user equilibrium model as follows:

$$\min \sum_{d\in D}\sum_{m\in M}\int_0^{q^d_m}\left(\frac{1}{\theta_d}\ln\frac{w}{q_d} + c^d_m(w) - \beta^d_m\right)\mathrm{d}w + \sum_{d\in D}\int_0^{q_d}\left(\frac{1}{\delta}\ln\frac{w}{Q} - \alpha_d\right)\mathrm{d}w, \tag{2a}$$

subject to

$$\sum_{d\in D} q_d = Q, \tag{2b}$$

$$\sum_{m\in M} q^d_m = q_d, \quad \forall d \in D, \tag{2c}$$

$$q_d \geq 0, \quad \forall d \in D, \tag{2d}$$

$$q^d_m \geq 0, \quad \forall d \in D, \forall m \in M, \tag{2e}$$

where θ_d is the impedance parameter associated with the travel mode choice to the destination region d, δ is the impedance parameter associated with destination choice, β^d_m is the exogenous attractiveness of the travel mode m to the destination d, and α_d is the exogenous attractiveness of the destination region d. q^d_m indicates travel demand in the travel mode m from Wuhan to the destination region d. q_d indicates travel demand from Wuhan to the destination region d. As to α_d, we develop the following weighted destination attractiveness measure to quantify the attractiveness of each destination to Wuhan:

$$\alpha_d = aH_d \cdot (L_d)^{k_d} + bP_d, \quad \forall d \in D, \tag{2f}$$

where H_d is the normalized historical demand distribution ratio of the destination region d; P_d is the normalized population of the destination region d; L_d is the normalized distance between the destination d and Wuhan; a is a weighting parameter for the parameter H_d; b is a weighting parameter for the parameter P_d; k_d is a weighting parameter for the parameter L_d. The weighting parameters a, b, and k_d reflect the extent of effects of historical demand distribution, population, and distance on the attractiveness of a destination region d. Learned from real-life experiences, the historical demand distribution ratio of a destination region d (H_d) is correlated oppositely to its travel distance to Wuhan (L_d). Furthermore, referring to equation (2l), for a destination region d, its generalized travel cost to Wuhan (u_d) varies incrementally with the travel time which is determined by the travel distance (L_d). To mitigate the interrelation between H_d and u_d, the term (aH_d) is multiplied by the term $(L_d)^{k_d}$.

We denote the original data of historical demand distribution ratio, population, and travel distance of a destination region d as h_d, p_d, and l_d. As h_d, p_d, and l_d are incommensurable, namely, all are measured in different units, they cannot be directly added and need to be normalized before the use of the weighted-sum method. To do so, we define H_d, P_d, and L_d as follows:

$$H_d = \frac{h_d}{\min(\mathbf{h_d})}, \quad \forall d \in D, \tag{2g}$$

$$P_d = \frac{p_d}{\min(\mathbf{p_d})}, \quad \forall d \in D, \tag{2h}$$

$$L_d = \frac{l_d}{\max(|\mathbf{l}|_{\mathbf{d}})}, \quad \forall d \in D, \tag{2i}$$

where $\min(\cdot)$ is a function to obtain the minimum item in a list, for example, $\min(|\mathbf{h}|_{\mathbf{d}})$ is to get the minimum item in the list $\mathbf{h_d}$. $\max(\cdot)$ is a function to obtain the maximum item in a list, for example, $\max(\mathbf{l_d})$ is to get the maximum item in the list $\mathbf{l_d}$. According to equation (2i), it is easy to get that $0 \leq L_d \leq 1$, from which we can infer that the value of the weighted distance parameter $(L_d)^{k_d}$ ranges from 0 to 1 for any k_d ($k_d > 0$). Besides, it can be learned from experiences

that passengers are more sensitive to travel cost in a short trip than in a long trip. This phenomenon has been studied in the area of stochastic traffic flow distribution [19]. In this work, passengers within the province of Hubei are more sensitive to the travel cost than those traveling out of the province of Hubei because of shorter travel distance. That is to say, the magnitude of travel cost takes a greater effect on the attractiveness of a destination region inside Hubei than that outside Hubei, meaning the value of $(L_d)^{k_d}$ should be greater for $d \in D_{\text{in}}$ than for $d \in D_{\text{out}}$. Along with the already known condition that $0 \le L_d \le 1$, it consequently requires the travel distance-related weighting parameter k_d taking a smaller value for $d \in D_{\text{in}}$ than $d \in D_{\text{out}}$. Furthermore, as the provincial capital of Hubei, Wuhan attracts a good many of migrant workers and students working or studying there each year for its abundant employment opportunities and diverse educational resources. The migrant population constitutes the majority of travel demands in the Spring Festival travel season in Wuhan. Without unexpected disruption, the historical traffic distribution of Wuhan in recent Spring Festival travel seasons will provide high-quality evidence for predicting the traffic distribution of this year. To reflect the significant impacts of the historical traffic distribution on the assessment of a destination's attractiveness, we suggest that the historical traffic distribution-related weighting parameter a takes a larger value than the population-related weighting parameter b. The detailed value setting for various parameters defined in this part can be found in Table 3.

The objective function (2a) is a two-level nested logit choice model to deal with the interrelated decisions in a multimodal network. The first level focuses on destination choice and the second level on mode choice. Equation (2b) ensures that the amount of flow assigned to different destination regions from Wuhan sums to the total travel demand Q which, in this work, amounts to 5,000,000. Equation (2c) represents the mode flow conservation constraint. Equations (2d) and (2e) are the nonnegativity conditions for destination demands and mode flows, respectively.

By deriving the first-order optimality conditions of the proposed program, we have the following nested logit model for destination choice and mode choice, respectively:

$$q_m^d = q_d \frac{\exp\left[-\theta_d\left(c_m^d - \beta_m^d\right)\right]}{\sum_{x \in M} \exp\left[-\theta_d\left(c_x^d - \beta_x^d\right)\right]}, \quad \forall d \in D, \forall m \in M, \tag{2j}$$

$$q_d = Q \frac{\exp\left[-\delta\left(u_d - \alpha_d\right)\right]}{\sum_{x \in D} \exp\left[-\delta\left(u_x - \alpha_x\right)\right]}, \quad \forall d \in D, \tag{2k}$$

where ud is users' perception of the generalized cost of traveling from the origin city Wuhan to the destination city d, which is computed as a "log-sum" of travel cost of each mode, i.e.,

$$u_d = -\frac{1}{\theta_d} \ln \sum_{m \in M} \exp\left[-\theta_d\left(c_m^d - \beta_m^d\right)\right], \quad \forall d \in D. \tag{2l}$$

To solve the nested logit model-based problem, one can first compute the generalized cost u_d $(\forall d \in D)$ according to equation (2l) and then carry out multiproportional traffic assignment (2j)-(2k) to obtain the combined destination distribution and modal split, i.e., q_m^d and q_d.

3. Case Study

The outbreak of COVID-19, which started in December last year, took Wuhan as the center and soon spread to all regions of China (including Hong Kong, Macao, and Taiwan). In the early morning of January 22, the province of Hubei launched level II emergency response to public health emergencies, and then cities in Hubei successively stopped public transportation. As of 11 : 00 on January 24, public transportation in 12 cities in Hubei had been shut down, including Wuhan, E'zhou, Xiantao, Zhijiang, Qianjiang, Huanggang, Chibi, Jingmen, Xianning, Huangshi, Dangyang, and Enshi, among which Wuhan, as the transport hub of more than 10 million people, temporarily closed its airports, rail stations, and all main roads out of town, as well as suspended public buses and subways. The government announced that citizens should not leave Wuhan without special reasons, and the lift of the lockdown will be announced separately. On January 26, the Information Office of the People's Government of Hubei held a press conference, pointing out that from the beginning of the Spring Festival to the closure of Wuhan, more than 5 million people left Wuhan, and more than 9 million remained in the city.

In this section, we will use the transportation model proposed in Section 2 to analyze the traffic flow distribution for the 5 million people outbound from Wuhan and then estimate the epidemic situation based on the demand distribution results. We are mainly concerned about the distribution of people within the province of Hubei as well as outside the province of Hubei. Figure 1 shows the map of the province of Hubei and 35 other regions of China, and Figure 2 shows the map of Wuhan and 16 other cities in the province of Hubei.

To facilitate the computation of the travel utility to a destination province outside Hubei, instead of calculating the travel utility to each city in the destination province, we only calculate the travel utility to the provincial capital city. For the calculation of the normalized historical demand distribution ratio parameter H_d in equation (2f), we collect the data of migration from Wuhan to other destination regions of the year 2017 on the Tencent social network's Spring Festival geographic positioning data platform. The data show that except several provinces including Henan, Hunan, Anhui, Jiangsu, and Guangdong, for other provinces, the majority of the traffic out of Wuhan flowed into their provincial capitals. As a result, we replace the population of a province by the population of its provincial capital for the computation of the parameter P_d in equation (2f). As to other five provinces, i.e., Henan, Hunan, Anhui, Jiangsu, and Guangdong, we use the sum of population of cities which occupied the most amount of immigration from Wuhan in 2017 instead of the population of the province. Besides, to obtain the travel distance parameter L_d in equation (2f), we use the road length from Wuhan to other destination regions to measure the travel distance. The data

Table 3: Parameters for nested logit model-based traffic assignment.

vot_{auto}	$vot_{\text{high-speed rail}}$	vot_{rail}	vot_{coach}	vot_{flight}
1.2	1.1	1.25	1.3	1.0
$\varepsilon_{\text{auto}}$	n	$\theta_d\,(\forall d \in D_{\text{in}})$	$\theta_d\,(\forall d \in D_{\text{out}})$	$\beta_m^d(\forall d \in D, \forall m \in M)$
0.6	2	0.05	0.01	0.0
δ	a	b	$k_d\,(\forall d \in D_{\text{in}})$	$k_d\,(\forall d \in D_{\text{out}})$
0.003	10	5	0.3	0.5

Figure 1: Wuhan and other 35 regions outside the province of Hubei.

Figure 2: Wuhan and other 16 cities in the province of Hubei.

of historical demand distribution, the population of cities and provinces, and the road distance from Wuhan to other destination regions can be found in Table 4. parameters for the computation of the nested logit model-based traffic assignment are listed in Table 3. Learned from the real traveling experiences, parameters are set as follows:

Table 4: The historical demand distribution data, the population of cities and provinces, and the road distance from Wuhan to other destination regions.

Destination	Historical demand distribution ratio	Population in millions	Road distance
Xiaogan	0.118615	4.8780	76.5
Huanggang	0.110331	6.2910	75.3
Jingzhou	0.055153	5.7442	220
Xianning	0.043188	2.4626	92.6
E'zhou	0.031015	1.0487	75
Xiangyang	0.036824	5.6140	313
Huangshi	0.033994	2.4293	100
Jingmen	0.029304	2.8737	240
Suizhou	0.028677	2.1622	170
Xiantao	0.029431	1.1660	102
Yichang	0.024785	4.1150	322
Tianmen	0.020131	1.4189	142
Enshi	0.016231	3.2903	519
Shiyan	0.017129	3.3830	443
Qianjiang	0.011413	0.9463	155
Hebei	0.01537	11.0312	898
Shanxi	0.00676	4.4619	944
Liaoning	0.00442	8.3160	1812
Jilin	0.00177	7.6770	2088
Heilongjiang	0.00246	10.8580	2354
Jiangsu	0.01780	25.3086	550
Zhejiang	0.01188	10.3600	827
Anhui	0.02734	24.5670	388
Fujian	0.00958	7.8000	919
Jiangxi	0.02451	5.5455	355
Shandong	0.01502	7.4604	864
Henan	0.07515	40.5440	514
Hunan	0.04200	32.6188	345
Guangdong	0.02316	45.9177	955
Hainan	0.00337	2.3023	1566
Sichuan	0.02397	16.3300	1130
Guizhou	0.00746	4.8819	1011
Yunnan	0.00627	6.8500	1558
Shanxi	0.01332	10.0037	740
Gansu	0.00433	3.7536	1360
Qinghai	0.00097	2.3871	1594
Beijing	0.01147	21.536	1174
Tianjin	0.00222	15.6183	1144
Shanghai	0.00792	24.2814	825
Chongqing	0.01638	31.2432	897
Inner Mongolia	0.00195	3.1260	1380
Guangxi	0.00840	7.5687	1209
Ningxia	0.00074	2.2931	3267
Xinjiang	0.00182	3.5058	1107

Note that, in this part, the unit of measurement is kilometers for the distance, minutes for the time, and CNY for all kinds of tolls and fees.

$0 < vot_{\text{flight}} < vot_{\text{high-speed rail}} < vot_{\text{auto}} < vot_{\text{rail}} < vot_{\text{coach}}$. Furthermore, in this study, we consider different travel cost sensitivities of passengers with different scale of travel path sizes. The related research results [19] reveal that passengers in short trip are more sensitive to travel distance or travel cost than those in long trip, which causes the value of θ_m^d for $\forall d \in D_{\text{in}}$ is 5 times that for $\forall d \in D_{\text{out}}$.

3.1. Demand Assignment. Based on the model proposed in Section 2, we calculate the traffic flows from Wuhan to other 48 destination regions which include 15 cities within Hubei, and 33 destination regions outside Hubei. Note that we exclude several regions which include the Shennongjia Forest District in Hubei, the Diaoyu Islands, and the South China Sea Islands from the calculation of destination demand distribution for that the traffic flows of these regions are very small. Besides, the demand distribution in real condition is collected from the Baidu Migration Big Data Platform. The error ratio of estimation is defined as the ratio of the estimation error to the result in real condition. Data of the estimated demand distribution, the demand distribution in real condition, and the error of estimation are listed in Tables 5 and 6 for cities within the province of Hubei and destination regions outside Hubei, respectively.

Table 5: Demand distribution estimation and the error of estimation for cities inside the province of Hubei.

Destination	Real condition	Est. results	Error	Error ratio (%)
Xiaogan	690000.00	665702.75	−24297.25	−3.52
Huanggang	652000.00	612343.63	−39656.37	−6.08
Jingzhou	327000.00	320223.65	−6776.35	−2.07
Xianning	250500.00	274428.51	23928.51	9.55
E'zhou	198500.00	235207.15	36707.15	18.49
Xiangyang	196500.00	193181.29	−3318.71	−1.69
Huangshi	188500.00	236658.71	48158.71	25.55
Jingmen	165000.00	156216.92	−8783.08	−5.32
Suizhou	160500.00	199004.52	38504.52	23.99
Xiantao	148500.00	202067.37	53567.37	36.07
Yichang	140500.00	131028.35	−9471.65	−6.74
Tianmen	104000.00	183119.51	79119.51	76.08
Shiyan	93000.00	89343.10	−3656.90	−3.93
Enshi	90500.00	64965.07	−25534.93	−28.22
Qianjiang	57000.00	140509.64	83509.64	146.51

Table 6: Demand distribution estimation and the error of estimation for other province-level destination regions outside the province of Hubei.

Destination	Real condition	Est. results	Error	Error ratio (%)
Henan	284000.00	250214.37	−33785.63	−11.90
Hunan	174000.00	187131.66	13131.66	7.55
Anhui	113500.00	144540.75	31040.75	27.35
Jiangxi	106000.00	128569.12	22569.12	21.29
Guangdong	97000.00	44218.78	−52781.22	−54.41
Jiangsu	73000.00	88634.88	15634.88	21.42
Chongqing	63500.00	42893.78	−20606.22	−32.45
Sichuan	62000.00	20641.30	−41358.70	−66.71
Shandong	55000.00	27805.30	−27194.70	−49.44
Zhejiang	53500.00	45031.19	−8468.81	−15.83
Hebei	46500.00	40775.05	−5724.95	−12.31
Fujian	45500.00	36048.21	−9451.79	−20.77
Beijing	43000.00	26050.15	−16949.85	−39.42
Guangxi	39500.00	14846.45	−24653.55	−62.41
Shanxi	36000.00	37590.59	1590.59	4.42
Shanghai	33000.00	36512.91	3512.91	10.65
Shanxi	29500.00	22472.40	−7027.60	−23.82
Guizhou	27500.00	21864.32	−5635.68	−20.49
Yunnan	26500.00	8502.62	−17997.38	−67.91
Hainan	19000.00	2387.83	−16612.17	−87.43
Gansu	17500.00	8962.46	−8537.54	−48.79
Liaoning	16500.00	2702.27	−13797.73	−83.62
Heilongjiang	14000.00	1237.75	−12762.25	−91.16
Xinjiang	10000.00	68.07	−9931.93	−99.32
Inner Mongolia	9000.00	6731.88	−2268.12	−25.20
Jilin	8500.00	1706.55	−6793.45	−79.92
Tianjin	7500.00	18275.56	10775.56	143.67
Ningxia	4000.00	3969.71	−30.29	−0.76
Qinghai	3000.00	3140.77	140.77	4.69
Tibet	1000.00	4156.12	3156.12	315.61
Others	19500.00	18317.04	−1182.96	−6.07

Table 7 provides the results of the aggregated demand distribution ratio, which shows that, in both the real and estimation conditions, the traffic flows within the province of Hubei account for most part (about 70%) of the total demands. It is also shown in Table 7 that the aggregated error ratio of demand estimation for cities inside Hubei (6.99%) is smaller than that for destinations outside Hubei (15.73%), meaning it performs better in demand estimation within the province of Hubei, and the aggregated error ratio of demand estimation for all destination regions is 18.60%. The demand distribution results which take a decreasing order are shown in Figure 3. The destination name marked with an asterisk denotes a city within the province of Hubei. Note that in Figure 3, we put the demand distribution results of Hong Kong, Macao, and Taiwan into one item named "others" for brevity. According to results in Figure 3, in both the real and estimation conditions,

Table 7: Results of the aggregated demand distribution ratio and the aggregated error ratio of the estimated demand distribution for all destinations, destinations inside Hubei, and destinations outside Hubei.

Destination range	Aggregated traffic distribution ratio		Aggregated error ratio of estimation (%)
	Real condition (%)	Estimation (%)	
All	—	—	18.60
Des. inside Hubei	69.24	74.08	6.99
Des. outside Hubei	30.76	25.92	15.73

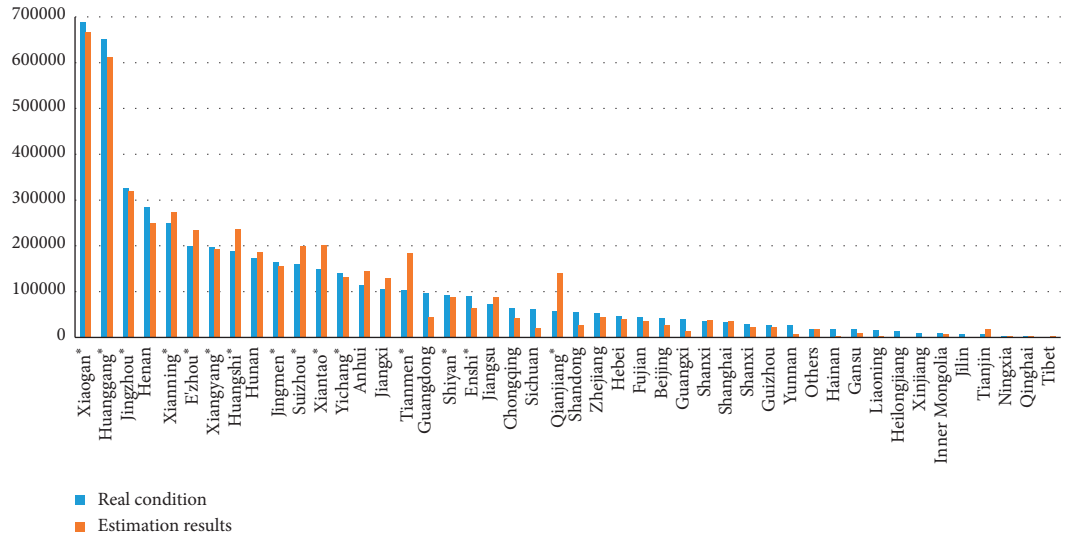

Figure 3: Traffic flow distribution results for the real condition.

Xiaogan, Huanggang, Jingzhou, Xianning, and E'zhou are the top five cities within the province of Hubei with the largest distribution of people, and Henan, Hunan, Anhui, and Jiangxi are the top four destination regions outside Hubei with the largest distribution of people. All results indicate that in a tolerable error range, our model delivers a desirable performance on the estimation of traffic flow distribution.

3.2. Numerical Estimation of Incidence Cases. According to statistics released by the Chinese health authority, after March 18, all the increased confirmed cases in China are imported from overseas. Therefore, we use statistics of the day, March 18, to obtain the number of confirmed cases resulted from the travelers from Wuhan. The average incidence rate (γ) of people leaving Wuhan is defined as follows:

$$\gamma = \frac{f}{5,000,000}, \tag{3a}$$

where f is the number of confirmed cases nationwide apart from Wuhan. With $f = 31296$, we have $\gamma = 0.6259\%$. We then further estimate the number of incidence cases in different destination regions which is equal to $q_d * \gamma, \forall d \in D$. Results of the real number of incidence cases, the estimated number of incidence cases, the error of estimation for the number of incidence cases as well as the error ratio estimation for the number of incidence cases are listed in Tables 8 and 9 for destinations within and outside Hubei, respectively.

Table 8: Estimation of the number of incidence cases and the error of estimation for cities inside the province of Hubei.

Destination	Real condition	Est. results	Error	Error ratio (%)
Xiaogan	3518.00	4166.77	648.77	18.44
Huanggang	2907.00	3832.78	925.78	31.85
Jingzhou	1580.00	2004.34	424.34	26.86
Xianning	836.00	1717.70	881.70	105.47
E'zhou	1394.00	1472.21	78.21	5.61
Xiangyang	1175.00	1209.16	34.16	2.91
Huangshi	1015.00	1481.29	466.29	45.94
Jingmen	928.00	977.79	49.79	5.37
Suizhou	1307.00	1245.61	−61.39	−4.70
Xiantao	575.00	1264.78	689.78	119.96
Yichang	931.00	820.13	−110.87	−11.91
Tianmen	496.00	1146.18	650.18	131.09
Shiyan	672.00	559.22	−112.78	−16.78
Enshi	252.00	406.63	154.63	61.36
Qianjiang	198.00	879.48	681.48	344.18

Figure 4 illustratively presents results in Tables 9 and 10. It can be observed from Figure 4 that our estimation overestimates the number of incidence cases in most cities within Hubei, as well as two provinces, i.e., Henan and Hunan. According to results in Section 3.1, these cities/provinces are the destination regions with the largest traffic flow distributions. The fact of the lower incidence rate of these destination regions with the most immigration from Wuhan than the average incidence rate implies that

Table 9: Estimation of the number of incidence cases and the error of estimation for other province-level destination regions outside the province of Hubei.

Destination	Real condition	Est. results	Error	Error ratio (%)
Henan	1274.00	1566.14	292.14	22.93
Hunan	1018.00	1171.29	153.29	15.06
Anhui	990.00	904.71	−85.29	−8.62
Jiangxi	936.00	804.74	−131.26	−14.02
Guangdong	1415.00	276.77	−1138.23	−80.44
Jiangsu	633.00	554.78	−78.22	−12.36
Chongqing	577.00	268.48	−308.52	−53.47
Sichuan	543.00	129.20	−413.80	−76.21
Shandong	768.00	174.04	−593.96	−77.34
Zhejiang	1238.00	281.86	−956.14	−77.23
Hebei	319.00	255.22	−63.78	−19.99
Fujian	313.00	225.63	−87.37	−27.91
Beijing	537.00	163.05	−373.95	−69.64
Guangxi	254.00	92.93	−161.07	−63.41
Shanxi	248.00	235.29	−12.71	−5.13
Shanghai	404.00	228.54	−175.46	−43.43
Shanxi	133.00	140.66	7.66	5.76
Guizhou	146.00	136.85	−9.15	−6.26
Yunnan	176.00	53.22	−122.78	−69.76
Hainan	168.00	14.95	−153.05	−91.10
Gansu	136.00	56.10	−79.90	−58.75
Liaoning	127.00	16.91	−110.09	−86.68
Heilongjiang	484.00	7.75	−476.25	−98.40
Xinjiang	76.00	0.43	−75.57	−99.44
Inner Mongolia	75.00	42.14	−32.86	−43.82
Jilin	93.00	10.68	−82.32	−88.51
Tianjin	141.00	114.39	−26.61	−18.87
Ningxia	75.00	24.85	−50.15	−66.87
Qinghai	18.00	19.66	1.66	9.21
Tibet	1.00	26.01	25.01	2501.40
Hong Kong	233.00	114.65	−118.35	−50.79
Macao	155.00	70.40	−84.60	−54.58
Taiwan	11.00	31.83	20.83	189.38

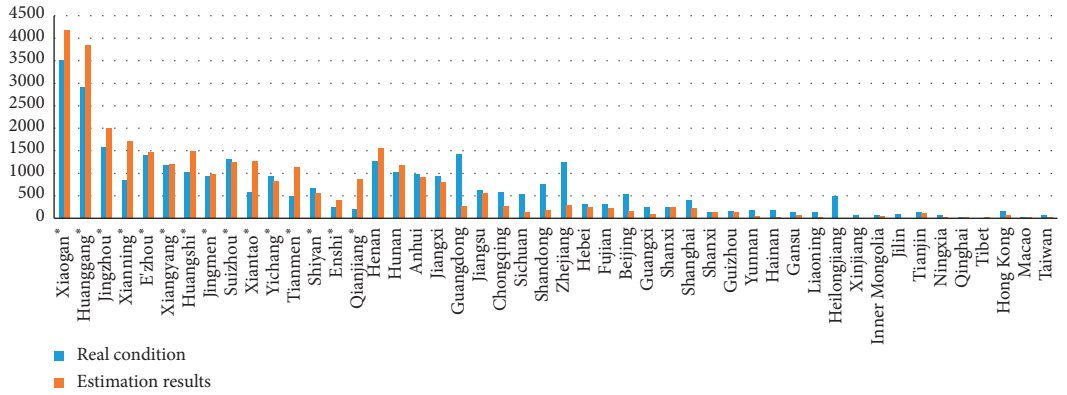

Figure 4: Comparison of the estimated number and the real number of incidence cases.

measures adopted by the Chinese government played an effective role in preventing a more serious situation from developing. Measures in the prevention and control of the epidemic involve lockdown on public transportations in 12 cities in Hubei, a two-week mandatory self-quarantine for people immigrated from Wuhan, residential community-based management, constructing temporary treatment centers, the centralized schedule of medical staff and supplies to the scarce areas, and so on. At the same time, results in Figure 4 also reveal that the model-based results underestimate the incidence rate of several destination regions including Guangdong, Chongqing, Sichuan, Shandong, Zhejiang, Beijing, Shanghai, Heilongjiang, and Hong Kong. This is because high frequent commercial activities that

Table 10: Mode flow distribution results of cities inside the province of Hubei.

City	Road	High-speed rail	Rail	Coach	Flight
Xiaogan	170285.59	178569.34	223626.44	93221.37	—
Huanggang	161473.63	25124.46	425745.54	—	—
Jingzhou	5018.37	45290.82	269914.25	0.22	—
Xianning	33196.64	151630.82	61341.02	28260.04	—
E'zhou	25378.08	188460.03	8447.63	12921.41	—
Xiangyang	3884.20	174498.63	14686.33	112.13	—
Huangshi	28096.44	200465.62	7468.12	628.54	—
Jingmen	129761.11	—	24305.32	2150.49	—
Suizhou	30586.40	155330.54	13007.88	79.70	—
Xiantao	87947.54	90625.94	—	23493.89	—
Yichang	29596.79	101257.41	94.67	79.47	—
Tianmen	26117.57	109137.47	47827.86	36.61	—
Shiyan	9449.63	79120.77	771.80	0.90	—
Enshi	5196.79	59325.61	441.77	0.90	—
Qianjiang	76189.15	62691.08	—	1629.41	—

involve face-to-face or close contact with other people lead to the higher incidence rates of the economically developed provinces, such as Guangdong, Zhejiang, Beijing, Shanghai, and Hong Kong. It is also interesting to see that the province of Heilongjiang, far away from Wuhan, not as commercially active as the provinces mentioned above, is featured by its high incidence rate. The high incidence rate of Heilongjiang may be attributed to the mass contact transmission of virus in gathering activities. According to news reported in Heilongjiang, to the date of February 7, there had been 48 family aggregating activities which were the source of 194 cases of cluster infection.

In Table 11, we compute the aggregated error ratio of estimation for the number of incidence cases which is equal to 39.52%, almost two times of the aggregated error ratio of estimation for the traffic flow distribution (18.60%), indicating that the spread of the epidemic is not linear with respect to the model-based traffic flow distribution. For cities within Hubei, the aggregated number of incidence case distribution ratio in real condition (56.40%) is much lower than the estimation (74.08%) while for provinces outside Hubei, the aggregated number of incidence case distribution ratio in real condition (43.60%) is much higher than the estimation (25.92%). This is because the spread of disease within Hubei is well controlled by means of transport restriction, medical assistance, and other effective methods while the high economic activity frequency as well as the high occurrence of mass gatherings in some provinces outside Hubei will potentially increase the incidence rate outside Hubei.

3.3. Mode Flow Distribution. Public transport as the main mode of transportation in big cities carries the highest risk of transmission of infection for a number of reasons. The high density of passengers confined in relatively small spaces was the primary cause. Besides, the in-vehicle air conditioning system featured by the low ventilation rates makes it easy for virus to spread. And the indirect infection from the contaminated public facilities in transport vessels is also one of the major danger sources. Furthermore, for passengers taking a long trip, multiple public transportation transfers are often involved, the fact of which potentially increases the incidence rate. In contrast, self-driving or taking a ride in a privately owned vehicle has several advantages over public transport in containing the transmission of infection. First, passengers are separated by vehicles. The spatial isolation reduces the risk of cross infection. Second, in the self-driving travel mode, passengers drive to destinations directly without any transfer most of the time. Third, people who are friends or familiar with each other often travel together in a privately owned vehicle. It is easy for them to learn the health condition of each other which helps to raise their awareness of health security and as a result mitigates the risk of infection. Comparisons of different transportation means' impacts on the virus spreading reveal that it is important to enhance the epidemic prevention from the perspective of public transport control.

In this section, we first calculate the mode flow distribution based on the proposed model. The mode flow distributions of each destination region are listed in Tables 10 and 12. The results of the aggregated mode flow ratio for destinations inside Hubei as well as outside Hubei are shown in Figure 5. It can be seen from Figure 5 that, for destinations both inside and outside Hubei, public transports are the mainstream transportation means accounting for about 80% of the total demands. Besides, the most popular travel mode of public transport is the high-speed railway for trips both inside and outside Hubei, which indicates that enhanced measurements, such as disinfection and disease detection, should be adopted by the high-speed railway transportation system. Furthermore, the proportion of aggregated mode flow ratio of the common railway inside Hubei (29.63%) is much higher than that outside Hubei (13.55%), indicating that, for trips from Wuhan to cities inside Hubei, extra efforts should also be paid on the epidemic control in the common railway transportation system.

To contain the COVID-19 outbreak, many countries have implemented flight restrictions to China. At the same time, China itself has imposed a lockdown of the transportation system of Wuhan as well as the entire Hubei province. In this context, it is reasonable to investigate how

Table 11: Results of the aggregated number of incidence case distribution ratio and the aggregated error ratio of the number of estimated incidence case distribution for all destinations, destinations inside Hubei, and destinations outside Hubei.

Destination range	Aggregated number of incidence case distribution ratio		Aggregated error ratio of the estimation (%)
	Real condition (%)	Estimation (%)	
All	—	—	39.52
Within Hubei	56.40	74.08	30.36
Outside Hubei	43.60	25.92	39.94

Table 12: Mode flow distribution results of other province-level destination regions outside the province of Hubei.

Destination	Road	High-speed rail	Rail	Coach	Flight
Henan	44850.03	118548.74	81885.68	4929.93	—
Hunan	39450.61	92948.86	43774.41	10957.78	—
Anhui	32300.71	107671.97	—	4568.06	—
Jiangxi	28926.26	82248.90	13420.05	3973.91	—
Guangdong	5998.14	36177.92	2020.71	21.68	0.33
Jiangsu	16969.83	70065.96	—	1599.09	—
Chongqing	3815.81	26847.00	12063.14	166.99	0.84
Sichuan	4396.64	15655.80	343.30	115.42	130.14
Shandong	16523.83	6598.24	3179.75	345.35	1158.13
Zhejiang	5446.38	36087.67	1047.02	255.62	2194.49
Hebei	3402.03	26799.17	10573.71	—	0.13
Fujian	3006.54	29630.07	1349.57	346.38	1715.65
Beijing	1164.38	21849.67	2971.85	64.20	0.05
Guangxi	1994.34	10993.61	1415.26	25.41	417.83
Shanxi	21077.62	13574.76	131.76	2740.70	65.76
Shanghai	7129.73	28941.40	113.64	328.00	0.13
Shanxi	4241.40	5456.97	1.04	258.44	12514.56
Guizhou	2971.35	17850.25	164.81	24.04	853.86
Yunnan	122.45	8364.34	5.24	0.08	10.50
Hainan	2237.15	—	26.92	26.92	96.83
Gansu	978.49	7754.39	36.45	3.31	189.81
Liaoning	183.87	2345.41	149.94	2.56	20.50
Heilongjiang	33.87	751.06	267.06	—	185.77
Xinjiang	2.69	—	1.79	—	63.58
Inner Mongolia	1385.89	—	0.02	—	5345.97
Jilin	22.74	1600.39	23.20	—	60.22
Tianjin	2057.90	15236.40	689.83	38.92	252.51
Ningxia	2615.52	—	2.36	—	1351.83
Qinghai	545.38	—	—	—	2595.38
Tibet	—	—	—	—	4156.12
Hong Kong	2933.43	8307.63	—	—	6.39
Macao	4666.53	—	—	—	419.13
Taiwan	—	—	—	—	1983.93

the mode flow distribution changes with different outbound transport restrictions in Wuhan. We will use the proposed nested logit model to analyze the role of lockdown on each transport means in the following content.

3.3.1. Lockdown Test. Table 13 shows the results of the aggregated demands ratio inside Hubei under cases applying lockdown on different travel modes and it reveals that a lockdown on any travel mode will lead to an increase of the aggregated demands ratio inside Hubei, among which shutting down the high-speed railway will cause the maximum rise of the aggregated demands ratio inside Hubei from 73.87% to 78.15%. This indicates that a lockdown on any travel mode will not make a big difference to the change of the aggregated demand distribution between destinations inside and outside Hubei. We then check the effects of transport restriction on the change of mode flow distribution, and related results are listed in Tables 14 and 15 for destinations inside Hubei and outside Hubei, respectively. From Tables 14 and 15, it can be seen that, for destinations both inside and outside Hubei, lockdown on a certain transportation means leads to the growth of traffic flows of other travel modes, and particularly lockdown on the high-speed railway has the most prominent impact on the traffic flow increment of other travel modes, indicating that in the

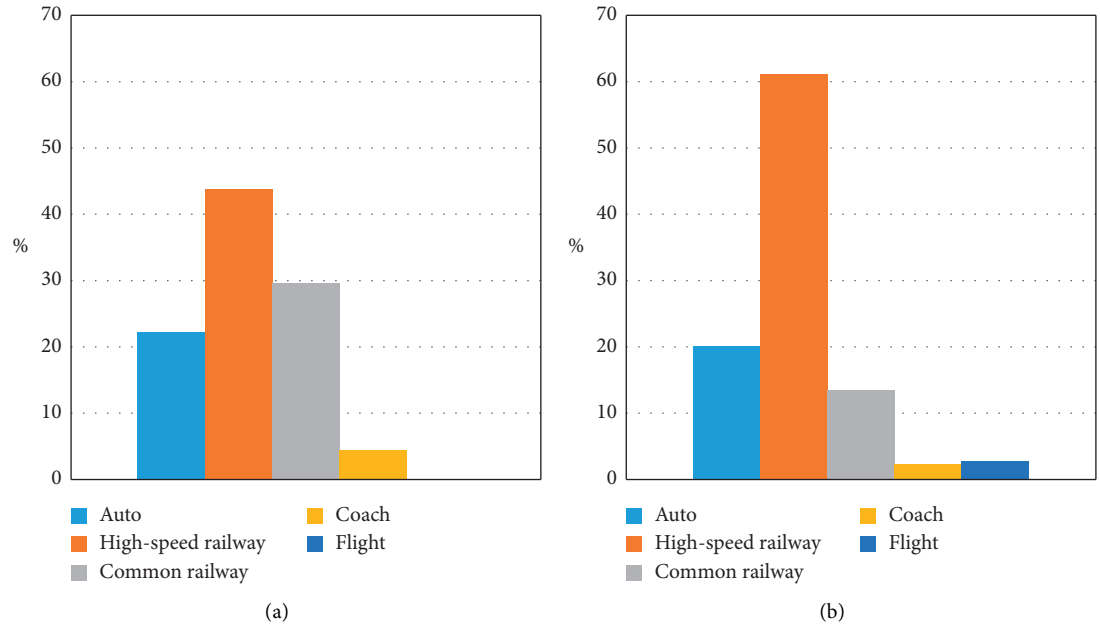

Figure 5: Aggregated mode flow distribution ratio of destination regions: (a) inside Hubei and (b) outside Hubei.

Table 13: Results of the aggregated traffic flow ratio of cities inside Hubei under cases applying lockdown on different travel modes.

Original case (%)	Locked down travel mode				
	Automobile (%)	High-speed railway (%)	Common railway (%)	Coach (%)	Flight (%)
74.08	75.06	78.63	74.41	74.16	74.34

Table 14: Results of the aggregated mode flow increment in percentage under cases applying lockdown on different travel modes for destinations inside Hubei.

Aggregated mode flow increment (%)	Locked down travel mode			
	Automobile (%)	High-speed railway (%)	Common railway (%)	Coach (%)
Automobile	—	121.59	63.65	5.49
High-speed railway	25.54	—	32.78	4.31
Common railway	35.29	62.22	—	4.02
Coach	42.98	102.42	36.47	—

Table 15: Results of the aggregated mode flow increment in percentage under cases applying lockdown on different travel modes for destinations outside Hubei.

Aggregated mode flow increment (%)	Locked down travel mode				
	Automobile (%)	High-speed railway (%)	Common railway (%)	Coach (%)	Flight (%)
Automobile	—	127.41	14.82	2.42	4.13
High-speed railway	19.98	—	14.34	1.94	1.37
Common railway	19.77	98.77	—	2.32	0.50
Coach	28.28	114.78	17.71	—	1.13
Flight	29.38	63.29	4.03	0.77	—

case of a lockdown on the high-speed railway, enforcement on the control of transportation exposures should be conducted for all the other public transport systems. It also reveals that a lockdown on a certain travel mode may cause different extent of aggregated mode flow increment of other travel modes. For example, the common railway restriction has the most significant impact on the increase of the aggregated mode flows of automobile (63.65%) for destinations inside Hubei. And the automobile restriction leads to higher aggregated mode flow growth of coach (42.98%) for destinations inside Hubei than any other aggregated mode flow increment. This indicates that it is important to measure the magnitude of correlation between lockdown on a certain travel mode and the traffic flow increase of other

Table 16: Derivatives of the aggregated mode flows of auto as well as the aggregated demands of destination regions with high incidence rates with respect to different input parameters.

Aggr. mode flow	$\partial(\cdot)/\partial P_{\text{highway}}$	$\partial(\cdot)/\partial \tau_{\text{high-speed rail}}$	$\partial(\cdot)/\partial \tau_{\text{rail}}$	$\partial(\cdot)/\partial \tau_{\text{coach}}$	$\partial(\cdot)/\partial \tau_{\text{flight}}$	$0.1 * \partial(\cdot)/\partial n$
Q_{auto}	−14934.37	16010.48	11616.38	2172.01	69.88	26895.38
$Q_{\text{high incidence}}$	21.96	−232.22	168.19	21.8	3.76	1954.73

travel modes, and the public transport mode which has a high correlation with the lockdown needs intensified management to contain virus spreading through transportation.

3.4. Sensitivity Analysis. In this work, the logit-based probability expression for both destination and mode choice ensures that the solution to the lower-level programming is unique. Hence, the standard sensitivity analysis method for nonlinear programming problem can be used directly to derive the sensitivity information. The detailed derivation can be referred to Yang and Chen [20] and Yang et al. [21]. In this section, we conduct sensitivity analyses to explore how changes in input parameters including road tolls, high-speed railway ticket fees, common railway ticket fees, coach ticket fees, flight ticket fees, and the average vehicle occupancy affect certain traffic flows we are interested in. To ease the work of analysis, we investigate the change of traffic flows with respect to the same amount of perturbations of a particular parameter for all destinations rather than for each destination, respectively. For example, the term of derivative $\partial(Q_{\text{auto}})/\partial P_{\text{highway}}$ indicates the change of the traffic flow Q_{auto} with respect to an increase of 1 Chinese Yuan (CNY) in the road tolls for all destinations, different from the derivative term $\partial(Q_{\text{auto}})/\partial P^{d}_{\text{highway}}$ $(\forall d \in D)$ which represents the change of the traffic flow Q_{auto} with respect to an increase of 1 CNY in the road toll for the specific destination indexed by d.

As aforementioned, compared with other public transport modes, traveling in privately owned vehicles contributes to less transportation exposures. As a result, measures taken to encourage traffic flows shifting from the public transport modes to the auto mode will mitigate transmission risks. We check the derivatives of the aggregated mode flows of auto which is defined as Q_{auto} with respect to perturbations of input parameters in Table 16. According to the results in Table 16, an increase of n has the most direct positive impact on Q_{auto}, which is followed by an increase of $\tau_{\text{high-speed rail}}$. This indicates that the increase of the average vehicle occupancy n and the increase of high-speed railway ticket fee $\tau_{\text{high-speed rail}}$ for all destinations are the most effective way to boost the aggregated mode flow of auto:

$$Q_{\text{high incidence}} = q_{\text{Zhejiang}} + q_{\text{Jiangsu}} + q_{\text{Guangdong}} + q_{\text{Beijing}} + q_{\text{Shanghai}} + q_{\text{Hong Kong}} + q_{\text{Heilongjiang}}. \tag{3b}$$

As we discussed in Section 3.2, the actual incidence rates in economically developed destinations as well as destinations with high occurrence of big gathering activities are much higher than the estimated incidence rates. It is a natural thought to prevent the virus spreading from seriously developing by curbing the demands of these destinations. The aggregated demands of the economically developed destinations as well as destinations with high occurrence of big gathering activities is defined as $Q_{\text{highincidence}}$ in equation (3b), which is the sum of demands of multiple destinations involving Zhejiang, Jiangsu, Guangdong, Beijing, Shanghai, Hong Kong, and Heilongjiang. We check the sensitivity of the aggregated demands of these destinations ($Q_{\text{high incidence}}$) with respect to different parameters in Table 16. One useful application of the derivatives of $Q_{\text{high incidence}}$ is to identify effective measures to induce negative growth of $Q_{\text{high incidence}}$. The negative value of $\partial Q_{\text{high incidence}}/\partial(\cdot)$ indicates that an increase in a particular parameter leads to a decline in $Q_{\text{high incidence}}$. In this study, decreasing n will cause the most decline in $Q_{\text{high incidence}}$, and the second largest decline is generated by increasing $\tau_{\text{high-speed rail}}$. These results indicate that the decrease of average vehicle occupancy as well as the increment of the high-speed railway pricing will be good candidates for the control of traffic flows from Wuhan to those destinations with high incidence rate risks. Remember that reducing n will also lead to a decrease of Q_{auto}, which is against the original aim of promoting the aggregated auto flows. This kind of contradictive effect of the adjustment of a certain parameter should be taken account of and considerate measures should be conducted. With the aim of increasing Q_{auto} and decreasing $Q_{\text{high incidence}}$ at the same time, we find a compromise in the conflict mentioned above, which raises the prices of high-speed railway tickets by a large amount while making a small improvement on the average vehicle occupancy or keeping the average vehicle occupancy without any change.

4. Conclusion

In this paper, a nested logit-based multimodal traffic flow distribution model and a solution algorithm are proposed. The model is designed taking account of experiences learned from historical data as well as making use of information collected from the real transportation system. The proposed model is verified by the application to a real-life problem of the demand distribution from Wuhan to other nationwide regions during the outbreak of COVID-19. The estimation results in the case show that the model proposed in this work delivers a desirable performance on demand distribution estimation. The results of the estimation of the number of incidence cases reveal that the spread of the epidemic is not linear with respect to the estimated traffic flow distribution results. And further analysis on this result inspires us that the

spread of the crisis is not purely dependent on the transportation situation, but also affected on the one hand by the control methods conducted by the public power and on the other hand by the frequency of local economic activities as well as the occurrence number of crowd-collected activities. The analysis of the role of lockdown on different travel modes reflects that lockdown on the high-speed railway has the most prominent impact on the traffic flow increment of other travel modes, and a lockdown on a certain travel mode causes different extent of aggregated mode flow increment of other travel modes. It is important to measure the magnitude of correlation between lockdown on a certain travel mode and the traffic flow increase of other travel modes. The public transport mode which has a high correlation with the lockdown policy needs intensified management to prevent virus from spreading through transportation. Furthermore, sensitivity analysis is implemented in this study, and based on the results of which, we work out a compromise solution for stimulating the traffic flow of automobile and reducing the demands of target regions with high incidence rates at the same time.

Data Availability

The data used to support this study are available at Tencent social network's 2017 Spring Festival geographic positioning data platform, Baidu Migration Big Data Platform (https://qianxi.baidu.com/2020/), and https://news.qq.com/zt2020/page/feiyan.htm#/global.

Conflicts of Interest

The authors declare that they have no conflicts of interest.

Acknowledgments

This work has been substantially supported by the National Natural Science Foundation of China through several projects (no. 71890970/71890973 and 71531011) and a project sponsored by the Program of Shanghai Academic Research Leader.

References

[1] R. M. Anderson, R. M. May, and B. Anderson, "The mathematics of infection. (Book reviews: infectious diseases of humans. dynamics and control)," *Science*, vol. 254, no. 2, pp. 591-592, 1991.

[2] N. Bailey, "The mathematical theory of infectious diseases and its applications," *Immunology*, vol. 34, no. 5, pp. 955-956, 1978.

[3] H. W. Hethcote, "The mathematics of infectious diseases," *SIAM Review*, vol. 42, no. 4, pp. 599–653, 2000.

[4] M. E. J. Newman, "The structure and function of complex networks," *SIAM Review*, vol. 45, no. 2, pp. 167–256, 2003.

[5] C. Li, W. Hu, and T. Huang, "Stability and bifurcation analysis of a modified epidemic model for computer viruses," *Mathematical Problems in Engineering*, vol. 2014, Article ID 784684, 14 pages, 2014.

[6] C. Fraser, C. A. Donnelly, S. Cauchemez et al., "Pandemic potential of a strain of influenza A (H1N1): early findings," *Science*, vol. 324, no. 5934, pp. 1557–1561, 2009.

[7] M. E. J. Newman, S. Forrest, and J. Balthrop, "Email networks and the spread of computer viruses," *Physical Review E*, vol. 66, no. 3, Article ID 035101, 2002.

[8] R. Pastor-Satorras and A. Vespignani, "Epidemic dynamics in finite size scale-free networks," *Physical Review E*, vol. 65, no. 3, Article ID 035108, 2002.

[9] Y. Wang, D. Chakrabarti, C. Wang, and C. Faloutsos, "Epidemic spreading in real networks: an eigenvalue viewpoint," in *Proceedings of the 22nd International Symposium on Reliable Distributed Systems (SRDS'03)*, pp. 25–34, IEEE, Florence, Italy, October 2003.

[10] D. Chakrabarti, Y. Wang, C. Wang, J. Leskovec, and C. Faloutsos, "Epidemic thresholds in real networks," *ACM Transactions on Information and System Security*, vol. 10, no. 4, pp. 1311–1326, 2008.

[11] I. Otero-Muras, G. Szederkényi, K. M. Hangos, and A. A. Alonso, "Dynamic analysis and control of biochemical reaction networks," *Mathematics and Computers in Simulation*, vol. 79, no. 4, pp. 999–1009, 2008.

[12] G. Pang and L. Chen, "Dynamic analysis of a pest-epidemic model with impulsive control," *Mathematics and Computers in Simulation*, vol. 79, no. 1, pp. 72–84, 2008.

[13] C. Jin and X.-Y. Wang, "Analysis and control stratagems of flash disk virus dynamic propagation model," *Security and Communication Networks*, vol. 5, no. 2, pp. 226–235, 2012.

[14] X. Y. Huang, C. Jin, and S. L. Jin, "Dynamic propagation model of blue-tooth virus on smart phones," *Advanced Materials Research*, vol. 121-122, pp. 620–626, 2010.

[15] Y. H. Li, J. X. Pan, and Z. Jin, "Dynamic modeling and analysis of the email virus propagation," *Discrete Dynamics in Nature and Society*, vol. 2012, Article ID 472072, 22 pages, 2012.

[16] M. Jackson and B. M. Chen-Charpentier, "A model of biological control of plant virus propagation with delays," *Journal of Computational and Applied Mathematics*, vol. 330, pp. 855–865, 2017.

[17] F. Jia and G. Lv, "Dynamic analysis of a stochastic rumor propagation model," *Physica A: Statistical Mechanics and Its Applications*, vol. 490, pp. 613–623, 2018.

[18] J. Zhang, J. Jiang, Y. Chen, K. Yang, H. L. You, and Y. W. Chen, "Epidemic spreading characteristics and immunity measures based on complex network with contact strength and community structure," *Mathematical Problems in Engineering*, vol. 2015, Article ID 316092, 10 pages, 2015.

[19] S. Kitthamkesorn and A. Chen, "A path-size weibit stochastic user equilibrium model," *Transportation Research Part B: Methodological*, vol. 57, no. 11, pp. 378–397, 2013.

[20] C. Yang and A. Chen, "Sensitivity analysis of the combined travel demand model with applications," *European Journal of Operational Research*, vol. 198, no. 3, pp. 909–921, 2009.

[21] C. Yang, A. Chen, X. Xu, and S. C. Wong, "Sensitivity-based uncertainty analysis of a combined travel demand model," *Transportation Research Part B: Methodological*, vol. 57, pp. 225–244, 2013.